Journal of Thermal Analysis, Vol. 44 (1995) 1449-1462

THERMAL, SPECTROSCOPIC AND XRD STUDIES ON NITROAMINOGUANIDINE (NAG)

S. R. Naidu, N. M. Bhide, K. V. Prabhakaran and E. M. Kurian

High Energy Material Research Laboratory, Pune-411021, India

(Received January 15, 1994; in revised form July 8, 1994)

Abstract

Nitroaminoguanidine (*NAG*) has been investigated as regards its thermal decomposition characteristics using simultaneous thermal analysis, infrared spectroscopy, X-ray diffraction and polarising microscopy. XRD studies show that *NAG* crystal belongs to the tetragonal system. The crystal structure parameters are found to be: $a=17.063\pm0.005$Å, $b=17.063\pm0.005$Å, $c=5.155\pm0.005$Å and c/a axial ratio $=0.302$. Under non-isothermal conditions, *NAG* decomposed apparently in one stage with a loss in weight of 80%. But the thermal decomposition of *NAG* in the solid phase under isothermal conditions proceeded through three stages. Both the first and the second stages obeyed the $A-E$ (Avrami Erofee'v) equation for $n=1$. The 3rd stage is too slow and kinetics has not been attempted. The rate parameters for the first and second stages have been evaluated. Gaseous decomposition products detected using the IR gas cell are NH_3, NO_2, HCN, N_2O, CO and CO_2. High temperature IR studies indicate preferential deamination reaction initially indicating breaking of $N-NH_2$ and $C-NH_2$ bonds leading to NH_2 radical formation. Addition of diphenylamine, a known chain inhibitor, decelerated the thermal decomposition, supporting a radical chain reaction.

Keywords: crystal structure, nitroaminoguanidine

Introduction

Guanidine compounds are important both as explosives and propellant ingredients as they contain extremely high percentage of hydrogen and energetically combined nitrogen in comparison to carbon. Study of the thermal stability of some guanidine salts [1] using differential thermal analysis tends to show that the decomposition exotherm seems to depend on the cation and anion structures and is possibly related to the hydrolysis constant of the salts. The infrared spectra [2, 3] of these compounds are of interest because they contain hydrogen of type N–H–O and N–H and for the availability of many free electrons. For *NAG* the total energy, heat of combustion, heat of formation, the effect of rotation across N–N bonds in the values of certain physico chemical parameters have been studied [4]. The kinetics and mechanism of the thermal decomposition of

0368–4466/95/ $ 4.00
© 1995 Akadémiai Kiadó, Budapest
John Wiley & Sons, Limited
Chichester

guanidine salts have a bearing on the combustion and stability of propellants containing these salts. The present work has therefore been undertaken to determine the reaction dynamics of the thermal decomposition of *NAG* by thermal analysis, infrared spectroscopy, hot stage microscopy and XRD.

Experimental

Nitroaminoguanidine was synthesized from nitroguanidine and hydrazine hydrate [5]. The nitroaminoguanidine thus obtained was then purified by recrystallisation. The decomposition temperature was found to be 189°C (reported 190°C). The purity of the compound was confirmed by high pressure liquid chromatography (Du Pont 8800 with RI detector, Zorbax ODS column, mobile phase methanol:water (50:50)).

A simultaneous thermoanalyser, NETZSCH STA 409 was used for thermal analysis. Cylindrical Pt-10% Ir thermocups with Pt-Pt 10% Rh thermocouples forming an integral junction with the thermocup were used. Calcined alumina was used as the reference material in thermal analysis.

Evolved gas analysis was based on the scheme of gas density balance where the effluent products of the sample were carried to a thermal conductivity cell by the carrier gas, wherein the equilibrium of a wheatstone bridge is influenced by the pneumatic equilibrium in such a way that the output voltage of the detector is proportional to the concentration of the gaseous products in the thermal conductivity cell and the direction of the EGA effect is upward, if the density of the measuring gas is more than that of the reference gas and vice versa.

In isothermal thermogravimetry, the sample (10 mg) was taken in the sample holder and the temperature was raised to the desired level using programmed heating of 10 deg·min^{-1} with a smooth gradual transformation from dynamic to the desired isothermal temperature towards the end of the thermal cycle with no overshooting of the temperature from the desired level. This method ensured temperature equilibrium and uniformity and a smooth start without disturbing the equilibrium of the microbalance.

For IR study [6–9], Perkin-Elmer IR Spectrophotometer Model 683 with double beam ratio recording system, which generally require no correction for sample temperature, was used. The high temperature IR cell was fabricated in the laboratory [10].

It consists of a brass cylinder with a specimen holder and with facilities for programmed heating. The outer surface of the brass cylinder has flexotherm electric winding cord, insulated with mica. Any desired temperature upto 300°C could be achieved. Chromel-alumel thermocouple was used as a sensor and a universal temperature programmer cum controller of Stanton-Redcroft was used. The temperature consistency during the experiment was within

±0.5°C. The specimen in the form of a pellet of 16 mm in dia was held in position by brass holder in which the thermocouple was located.

IR spectra of the sample in KBr pellets were recorded at room temperature and then at desired isothermal temperature during decomposition at regular time intervals. Isothermal temperature was achieved by programmed heating and control as in iso TG and the same thermal cycle was repeated for a set of experiments. Time allowed for equilibration at each temperature was about three minutes. Scanning speed was kept medium so that the time required for full scale scanning from 4000 to 200 cm^{-1} was 3 min. A specially designed IR gas cell with KBr windows was used to study the gaseous decomposition products of the thermal decomposition.

Leitz orthoplan polarising microscope with hot stage was used under dynamic heating conditions to characterise the morphological sequence of decomposition. The photomicrographs were taken at a magnification of 300.

For X-ray powder diffraction study a Philips PW1390/PW 1394 diffractometer with microprocessor control, analog and digital output, vertical goniometer and a photomultiplier PW 1965/60 as detector, was used. Diffraction

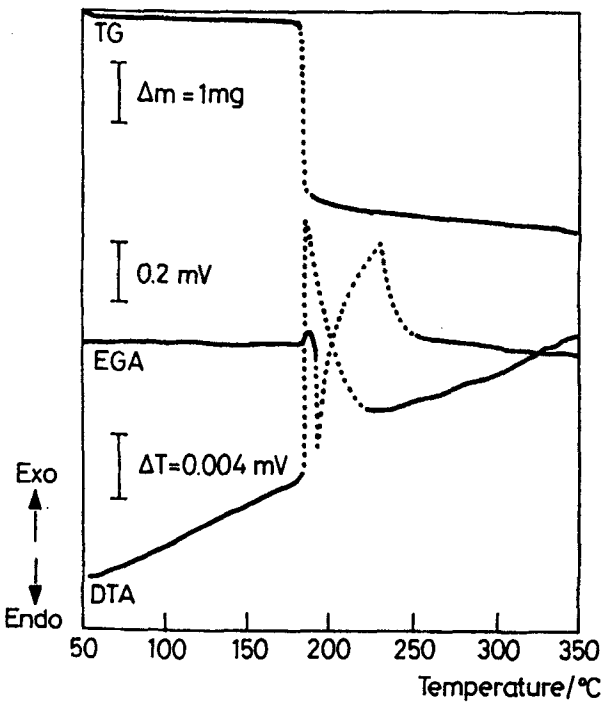

Fig. 1 TG–DTA–EGA of *NAG* under nitrogen atmosphere. Sample mass: 5 mg, particle size: 100 μ; heating rate: 10 deg·min^{-1}; reference gas: nitrogen 100 ml·min^{-1}; carrier gas – nitrogen 50 ml·min^{-1}; EGA bridge current: 100 mA; EGA sensitivity: 100%)

intensities *vs.* angle were recorded with nickel filtered CuK_α radiation (40 kV, 20 mA).

Results

Simultaneous thermogravimetry (TG), differential thermal analysis (DTA) and evolved gas analysis (EGA) of *NAG* were recorded under different conditions and a representative output is given in Fig. 1. TG shows apparently a single stage sharp weight loss of about 80% around 190°C followed by a gradual sluggish loss with the increase in temperature. DTA reveals two sharp exothermic peaks which overlap in the range 189–215°C indicating a two stage decomposition, followed by a slow change as indicated in TG. In EGA two gas evolution peaks are distinct in opposing directions in the range 189–240°C; this shift in temperature is due to the delay in carrying the evolved gas to the EGA detector cell. The first EGA peak in downward direction is attributed to the evolution of ammonia which is lighter than nitrogen, the reference gas used and the second in the opposite direction to the other denser gaseous products evolved subsequently in the second stage like oxides of nitrogen, carbon etc as listed in Table 3. At a heating rate of 20 deg·min^{-1}, in air atmosphere, the initial two stages are more pronounced and a third overall exotherm is revealed at about 400°C, vide Fig. 2. Interestingly these overlapping initial stagewise decomposition get resolved satisfactorily in TG under isothermal conditions in a narrow temperature band which was well below the onset of decomposition in dynamic TG making it feasible to attempt stagewise kinetics of thermal decomposition of *NAG*. At 153°C both the first and second stages involved a loss in weight of

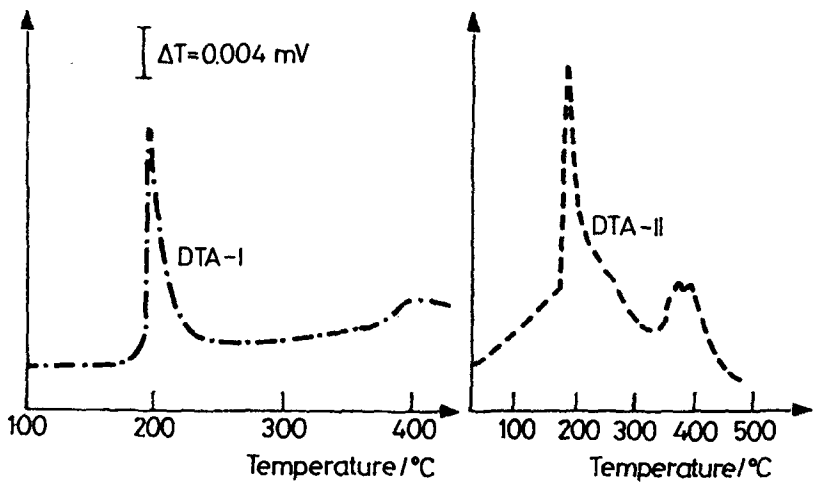

Fig. 2 DTA of *NAG* in air – Effect of heating rate. Sample mass: 5 mg, particle size: 100 μ; atmosphere: static air) DTA-I-10 deg·min^{-1}, DTA-II-20 deg·min^{-1}

about 25% each with respect to the initial weight of the sample and the third stage marginal loss in weight as indicated in the isothermal TG curve reproduced in the Fig. 3.

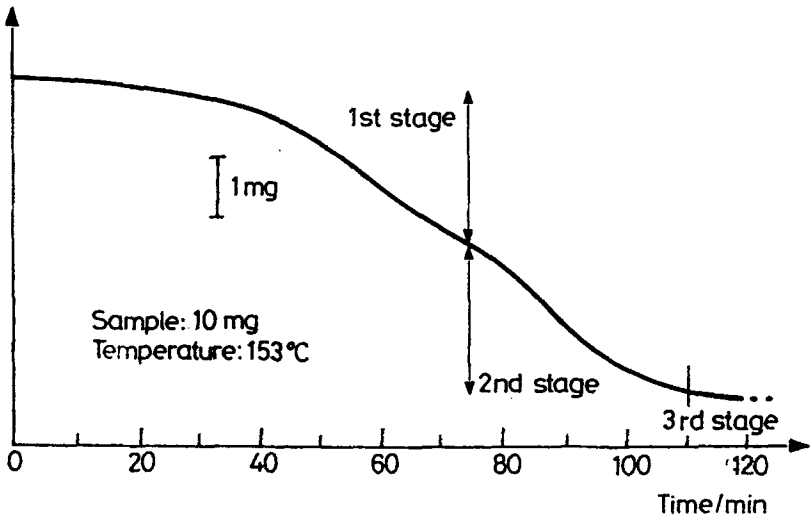

Fig. 3 Isothermal TG curve of *NAG* at 153°C

Kinetics of thermal decomposition

i) By isothermal TG

Isothermal TG of *NAG* was carried out in the range 150–173°C under static air. No initial reaction takes place while attaining these set isothermal temperatures as these are well below the onset temperature of about 189°C for decomposition for *NAG* in dynamic TG. The loss in weight of *NAG* at definite time intervals was measured from the respective isothermal TG curve. From these data the fraction decomposed, α, with respect to the original weight of the sample, in time, t, was calculated. The plot obtained for the first stage is given in Fig. 4, which is basically sigmoidal in nature. The decomposition has an induction period followed by a slow reaction, an acceleratory region and then a deceleratory one. For the second stage, α, was calculated with respect to the weight of the sample remaining after the first stage. α *vs.* t curve for this second stage is given in Fig. 5. The kinetics of the third stage was not studied, this being rather sluggish.

The α *vs.* t curves thus obtained were analysed using various rate equations [11–15], using a computer programme developed for these, to evaluate the rate constants. Close correlation was obtained between the Avrami-Erofee'v equa-

tion for $n=1$ and the contracting geometrical equations. AE equation for $n=1$, however gave a closer fit and the best linear Arrhenius plot for both the initial stages and hence was used for the evaluation of rate parameters given in Table 1.

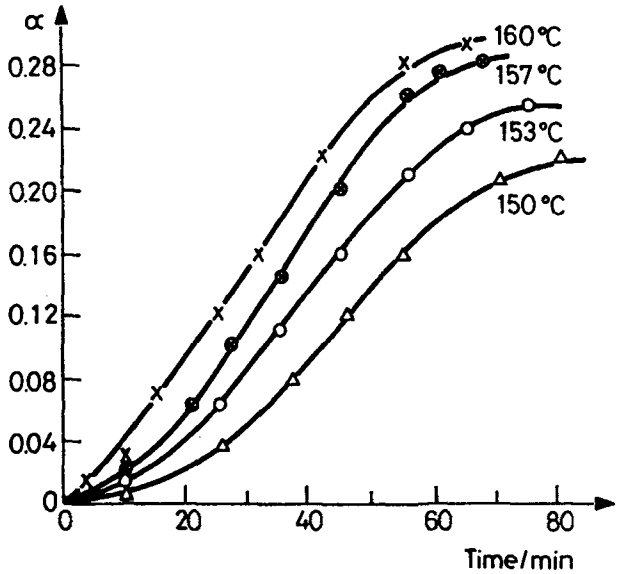

Fig. 4 α *vs. t* plot for the thermal decomposition of *NAG* (First Stage – isothermal TG)

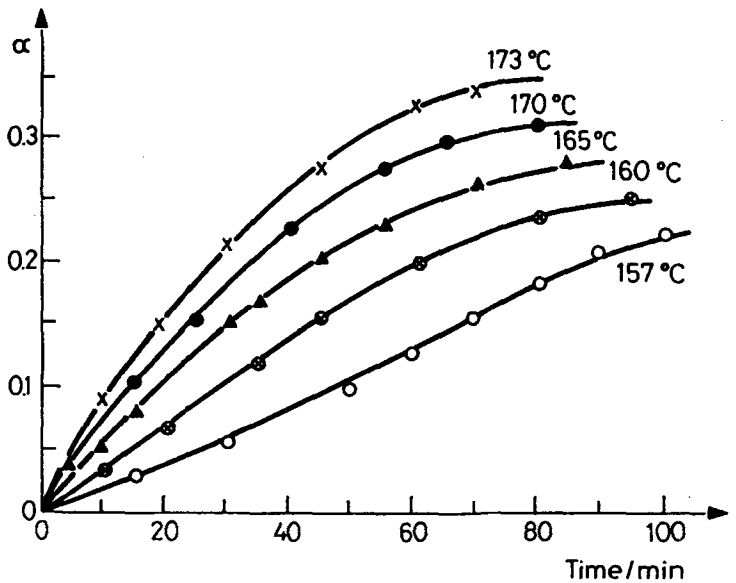

Fig. 5 α *vs. t* plot for the thermal decomposition of *NAG* (Second Stage – isothermal TG)

Table 1 Kinetic parameters for the thermal decomposition of nitroaminoguanidine

	Stage	Method	Energy of activation/ kJ·mole^{-1}	log A/ s^{-1}
I Fist stage				
i)	150–160°C	Isothermal TG	87.26	8.43
ii)	120–135°C	Isothermal IR	73.00	7.82
II Second stage				
i)	160–178°C	Isothermal TG	60.98	4.97
ii)	130–145°C	Isothermal IR (using $-NO_2$ band)	67.27	6.61
iii)	130–145°C	(using C=N band)	54.16	5.25

ii) Kinetics by IR spectroscopy

NAG is characterised [16–19] by the presence of prominent absorption bands at 1620 and 1675 cm^{-1} corresponding to the asymmetric stretching frequency for $-NO_2$ group and >C=N bond respectively and at 3200 cm^{-1} to 3410 cm^{-1} corresponding to symmetric and asymmetric stretching frequencies for the $-NH_2$ group.

Table 2 Variation of IR absorbance of $-NH_2$, $-NO_2$ and >C=N bands with temperature and time for *NAG*

Temperature/ °C		Time/ min		Loss of absorbance of the/%		
				$-NH_2$ band	$-NO_2$ band	C=N band
I	130	i)	0	–	–	–
		ii)	30	70	2	2
		iii)	60	95	4	4
II	135	i)	0	NIL	NIL	NIL
		ii)	20	60	24	19
		iii)	40	95	60	55
		iv)	60	–	90	80
		v)	80	–	95	95

The variation of band intensities, when followed as a function of temperature and time, (Fig. 6) was interesting, for these revealed preferential rate of loss of intensity as given in Table 2. The absorption intensity corresponding to $-NH_2$

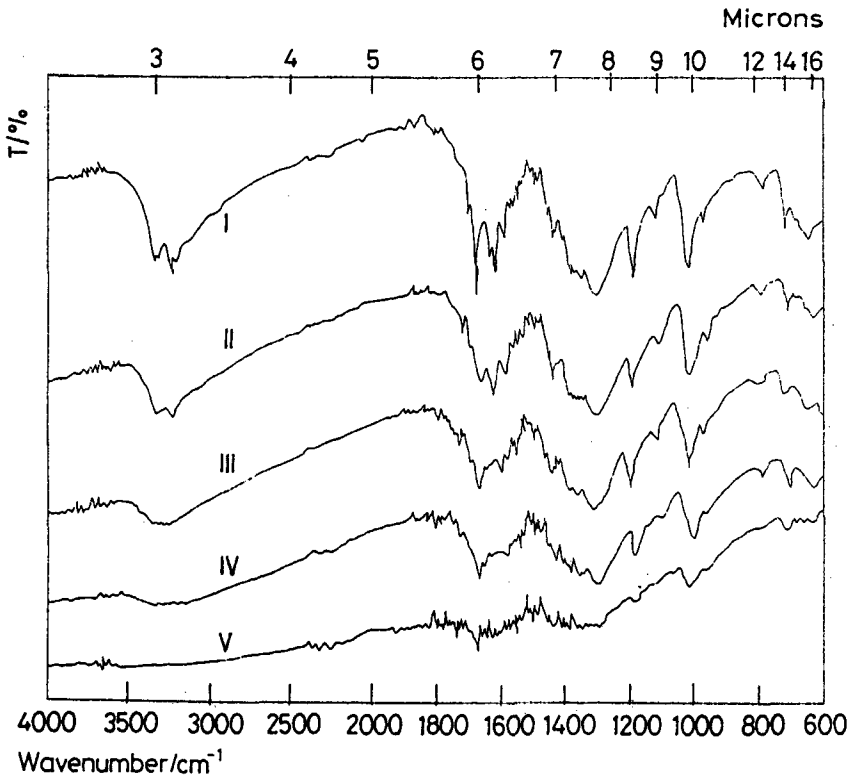

Fig. 6 IR Spectra of *NAG* at 135°C; I-'0' min, II-20 min, III-40 min, IV-50 min, and V-70 min

band decreased preferentially in the initial stage of thermal decomposition to those corresponding to $-NO_2$ and >C=N bands. The intensity loss due to the latter bands in fact was found to set in significantly after the disappearance of the $-NH_2$ bands. Therefore the thermal decomposition of *NAG* was followed [15, 20] using $-NH_2$ group frequency at 3410 cm^{-1} as well as $-NO_2$ and >C=N bands at 1620 and 1675 cm^{-1} respectively.

Absorbances of $-NH_2$, $-NO_2$ and >C=N bands in *NAG* for different concentrations were plotted which were found to be fairly linear indicating that all these absorption bands obey the Beer-Lamberts' law for *NAG*. The IR absorption band looses its intensity with increase in temperature. Therefore for calculation, the initial band intensity at the isothermal decomposition temperature has been taken as a measure of thermal initial concentration. The α *vs.* t plots thus obtained with respect to these functional groups are also sigmoidal in nature with an initial slow reaction followed by an acceleratory and then deceleratory stages and these also obeyed A-E equations for $n=1$. The rate parameters

obtained for the thermal decomposition of *NAG* using $-NH_2$, $-NO_2$ and >C=N bands are also given in Table 1. The difference in the E values as obtained by TG and IR may be due to the fact that TG gives the global kinetics while the IR gives specific kinetics with respect to the functional group used in the IR method.

Effect of additives

Effect of some additives on the kinetics of the thermal decomposition of *NAG* was studied using isothermal TG α *vs.* *t* plots for *NAG* mixed with carbamite, magnesium oxide, 2-nitro diphenylamine (*2NDPA*) and diphenylamine (*DPA*) each at 10% level at 165°C are given in Fig. 7. These show that *2NDPA*, carbamite and MgO accelerate the thermal decomposition of *NAG* but *DPA* decelerates it.

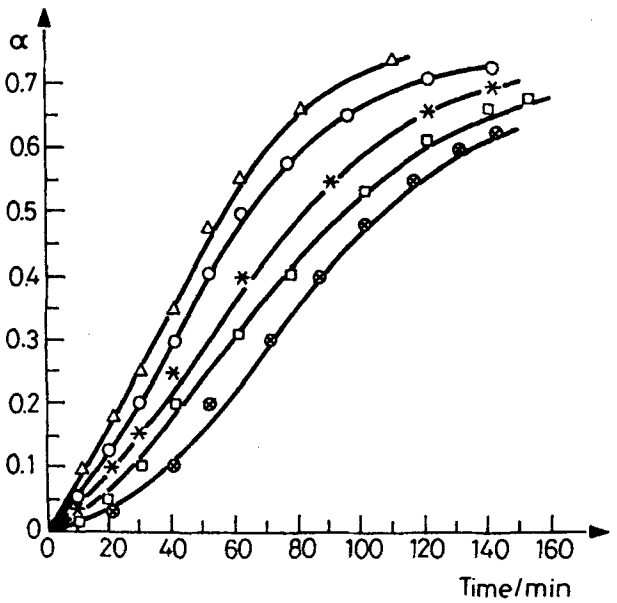

Fig. 7 α *vs.* *t* plot for the thermal decomposition of *NAG* - Effect of additives at 165°C
□*NAG*, **NAG*+Carbamite, o *NAG*+*2NDPA*, ⊗*NAG*+*DPA*, Δ *NAG*+MgO

Gaseous products by IR

Gaseous products evolved in the thermal decomposition of *NAG* were analysed [21] using thermal IR gas cell and these are given in Table 3.

Table 3 Gaseous thermolysis products of *NAG* by IR spectra

Wave number /cm^{-1}	Assignments
3340	NH_3
2350	CO
2330	CO_2
2230	N_2O
2200	CO
1640	NO_2
1270	N_2O
930	NH_3
970	NH_3
713	HCN
670	N_2O

Photomicroscopic studies

The thermal decomposition of *NAG* was also followed using hot stage microscopy to study the morphological changes occurring during the thermal decomposition. The photomicrographs obtained as a function of temperature and time are given in Fig. 8.

Microscopic studies on the thermal decomposition of *NAG* under dynamic temperature conditions reveal that *NAG* crystals gradually lose their transparency on heating. It did not show a clear cut melting. Above 180°C rapid crystal movements were observed. Evolution of gases sets in at this stage at localised points. These localised points later on developed into pipe holes whereby gaseous products bubbled out. The number of these pipe holes were found to increase leading to increased evolution of gas. A black charred residue was obtained at the end.

XRD

Crystal structure of *NAG*, it appears, has not yet been reported. XRD and refined crystal data of *NAG* calculated from Bragg angle, using a computer programme are given in Table 4. The results show that *NAG* crystal belongs to the tetragonal system.

Discussion

Thermal analysis results clearly indicate that the initial thermal decomposition of *NAG* proceeds in two stages and this is followed by a gradual sluggish stage.

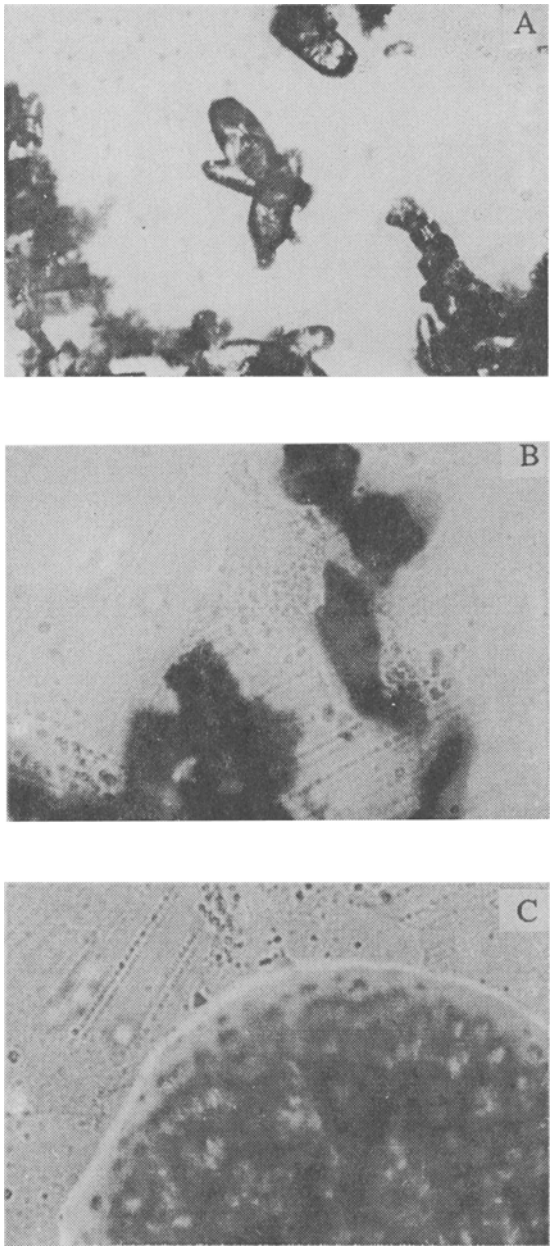

Fig. 8 Photomicrographs, I–III of *NAG* (×300). A – at room temperature; B – 185°C; C – 190°C

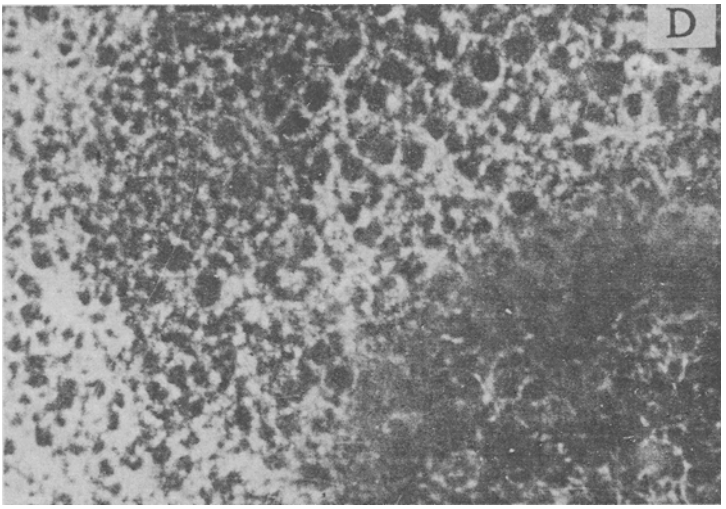

Fig. 8 Photomicrographs, IV of *NAG* (×300). D – at 195°C

In the thermal decomposition of *NAG* which has the nitramine molecular structure,

either N–N bond of hydrazine moiety, or N–NO_2 or C–NH_2 is expected to rupture initially. Rupture at the hydrazine linkage as well as C–NH_2 bond should lead to the formation of ·NH_2 radical [22]. The formation of ammonia as a gaseous product and also the preferential deamination of the parent molecule in the initial stage as shown by the high temperature IR studies, indicate N–N as well as C–NH_2 bond rupture [23, 24]. The primary process in the thermal decomposition of *NAG* may therefore be the rupture of N–N and C–NH_2 bonds leading to the formation of ·NH_2 radical.

IR spectroscopy indicates preferential loss of NH_2 absorbances in the first stage, while in the second stage those of the other important bands like –NO_2, >C=N etc. NO_2 and >C=N band intensity losses suggest N–NO_2 bond rupture leading to NO_2 free radical formation. And NO_2 has been identified as one of the main gaseous products in the second stage of thermolysis. This substantiates a radical chai nmechanism for the second stage also. *DPA*, a known chain inhibitor, decelerates the thermal decomposition of *NAG* further substantiates the radical chain mechanism proposed.

Table 4 Intensities, '*d*' values and refined crystal data of NAG calculated from Bragg angle (*c*/*a* axial ratio = 0.302) a = 17.063Å, b = 17.063Å, c = 5.155Å

Line No.	Bragg angle/θ	Intensity/ %	d*hkl* Å	Exptl. $\sin^2\theta$	Calcd. $\sin^2\theta$	d*hkl*
1	10.30	23	4.32	0.03197	0.03256	121
2	11.30	24	3.93	0.03839	0.03869	221
3	11.55	22	3.84	0.04008	0.04073	031
4	12.90	19	3.45	0.04981	0.04889	231
5	15.00	18	2.98	0.06669	0.06318	241
6	15.70	73	2.85	0.07322	0.07339	341
7	20.70	100	2.18	0.12490	0.12442	551
8	25.50	62	1.80	0.18534	0.18131	362
9	28.20	46	1.63	0.22330	0.22162	313

At macromolecular level, the reaction obeys Avrami–Erofee'v equation, for $n=1$ which implies that *NAG* undergoes thermal decomposition by random nucleation followed by unidimensional growth. Rate parameters obtained are in conformity with the reaction mechanism proposed.

References

1 Yuon P. Chringnan and D. R. Stariana, J. Org. Chem., 32 (1964) 285.
2 E. Lieber, D. R. Lering and L. J. Patterson, Anal. Chem., 23 (1951) 1593.
3 W. D. Kumbler and P. T. Peter., J. Org. Chem., 18 (1953) 669.
4 McEwari and M. W. Rigg, J. Chem. Soc., 73 (1951) 4725.
5 R. A. Henry, G. Mackosky, C. G. Robert and B. L. Smith, J. Amer. Chem. Soc., 73 (1951) 474.
6 K. C. Hartman and I. C. Hisastune, J. Phys. Chem., 69 (1965) 583.
7 Ibid 71 (1967) 392.
8 Henry A. Sent and Brawford Jr. J. Amer. Chem. Soc., 79 (1957) 1793.
9 R. W. Philips, J. Phys. Chem., 59 (1955) 1034.
10 S. R. Naidu, M. Sc. Thesis 'Solid State reactivity of high energy materials – studies on the solid state reactivity of some guanidine compounds' Pune University, 1986.
11 E. G. Prout and F. C. Tompkins, Trans. Farad. Soc., 40 (1944) 488.
12 M. Avrami, J. Chem. Phys. 7 (1939) 1103.
13 K. L. Mampel, J. Phys. Chem., (1940) 235.
14 E. M. Kurian, J. Thermal Anal., 35 (1989) 1111.
15 K. V. Prabhakaran, N. M. Bhide and E. M. Kurian, Thermochim. Acta, (in press).
16 L. J. Bellamy 'Advances in Infrared group frequency' Mathuen & Co. Ltd. London, 1968.
17 L. J. Bellamy 'The Infrared spectra of complex molecules' Chapman & Hall, London 1975.
18 C. N. R. Rao, Chemical application of infrared spectroscopy, Academic Press, New York 1963.
19 B. Franck, M. Horman and S. Schaibe, Chem. Ben., 90 (1957) 330.
20 K. Raha, P. S. Makashir and E. M. Kurian, J. Thermal Anal., 35 (1989) 1173.

21 H. Raymond Pierson, N. Aaron Fletcher and E. Stolair Gnatz. Anal. Chem., 28 (1956) 1219.
22 E. G. Janzen, J. Amer. Chem. Soc., 87 (1965) 3531.
23 K. K. Kuo and M. Summerfield (ed.) Fundamentals of solid propellant combustion, AIAA Inc. New York, VA 90, 1984, p. 215.
24 N. M. Bhide, S. R. Naidu, E. M. Kurian and K. R. K. Rao, J. Thermal Anal., 35 (1989) 1181.

Zusammenfassung — Mittels simultaner Thermoanalyse, Infrarotspektroskopie, Röntgendiffraktion und Polarisationsmikroskopie wurde die thermische Zersetzung von Nitroaminoguanidin (*NAG*) untersucht. Die Röntgendiffraktionsuntersuchungen ergaben, daß das *NAG*-Kristall dem tetragonalen System angehört. Die ermittelten Gitterkonstanten lauten: $a=17.0630.005$Å, $b=17.0630.005$Å, $c=5.1550.005$Å und das Achsverhältnis $c/a=0.302$. Unter nichtisothermen Bedingungen zersetzt sich *NAG* anscheinend in einem Schritt und verliert 80% seines Gewichtes. Dagegen verläuft die thermische Zersetzung von *NAG* in der Feststoffphase unter isothermen Bedingungen in drei Schritten. Sowohl der erste als auch der zweite Schritt unterliegen der *A-E* (Avrami Erofeev)-Gleichung für $n=1$. Der dritte Schritt verläuft zu langsam und die Kinetik konnte nicht erfaßt werden. Für den ersten und zweiten Schritt wurden die Geschwindigkeitsparameter abgeleitet. Die mittels einer IR-Gaszelle festgestellten gasförmigen Zersetzungsprodukte sind NH_3, NO_2, HCN, N_2O, CO und CO_2. IR-Untersuchungen bei hohen Temperaturen zeigen eine bevorzugte Deaminierungsreaktion, die zuerst auf die Spaltung der N–CH_2- und der C–NH_2-Bindung hinweisen, was zur Bildung von NH_2-Radikalen führt. Der Zusatz von Diphenylamin, eines bekannten Ketteninhibitors, verlangsamt die thermische Zersetzung und unterstützt eine radikalische Kettenreaktion.